Virology 485 (2015) 135–144

Contents lists available at ScienceDirect

Virology

journal homepage: www.elsevier.com/locate/yviro

HP-PRRSV is attenuated by de-optimization of codon pair bias in its RNA-dependent RNA polymerase nsp9 gene

Li Gao [a,1], Lianghai Wang [b,c,1], Chen Huang [b,c], Longlong Yang [e], Xue-Kun Guo [b,c], Zhibin Yu [b,c], Yihao Liu [b,c], Peng Yang [d], Wen-hai Feng [b,c,*]

[a] China Academy of Medicine Sciences, Peking Union Medical College, Institute of Medicinal Plant Development, Beijing 100193, China
[b] State Key Laboratory of Agrobiotechnology, Department of Microbiology and Immunology, College of Biological Sciences, China Agricultural University, Beijing 100193, China
[c] Department of Microbiology and Immunology, College of Biological Sciences, China Agricultural University, Beijing 100193, China
[d] Beijing Senkang Biotech Development Co., Ltd, Beijing 101400, China
[e] The Hamner Institutes for Health Sciences, Research Triangle Park, NC 27709-2137, USA

ARTICLE INFO

Article history:
Received 24 April 2015
Returned to author for revisions
21 May 2015
Accepted 16 July 2015
Available online 4 August 2015

Keywords:
Codon pair bias
Attenuation
HP-PRRSV
RNA dependent RNA polymerase
Vaccine

ABSTRACT

There is an urgent need to develop new vaccines against highly pathogenic PRRS virus (HP-PRRSV) variant in China. The actual use of each codon pairs is more or less frequent than that of the statistical prediction and codon pair bias (CPB) usage affects gene translation. We "shuffled" the existing codons in HP-PRRSV genes GP5, M, nsp2 and nsp9, so that the CPB of these genes could be more negative. De-optimization of nsp9, the RNA-dependent RNA polymerase, significantly decreased PRRSV replication in porcine alveolar macrophages (PAMs). *In vitro* study showed that HV-nsp9^{min} and HV-nsp29^{min} were remarkably attenuated in PAMs, and inoculation of pigs with 2 ml$*10^{5.0}$ $TCID_{50}$/ml of HV-nsp9^{min} or HV-nsp29^{min} did not cause PRRS. Importantly, pigs immunized with HV-nsp29^{min} were fully protected against different HP-PRRSV strains' lethal challenges. Our results imply that the CPB de-optimized HV-nsp29^{min} has the potential to be used as a live vaccine candidate against HP-PRRSV.

Introduction

Porcine reproductive and respiratory syndrome (PRRS) is one of the most important diseases in the swine industry (Neumann et al., 2005; Nieuwenhuis et al., 2012; Tian et al., 2007). It is estimated that the losses associated with PRRS are approximately $664 million per year in the United States alone (Neumann et al., 2005). Most recently, there have been devastating outbreaks of atypical PRRS in China and neighboring countries with a mortality of 20 to 100% (Li et al., 2007; Zhou et al., 2008), which is caused by a highly pathogenic PRRSV (HP-PRRSV) variant with an unique molecular hallmark, namely a discontinuous deletion of 30 amino acids in nonstructural protein 2 (nsp2). Currently, vaccination is generally used to control atypical PRRS. However, the available vaccines for HP-PRRSV are known to have drawbacks.

The etiological agent, PRRS virus (PRRSV), is a ~15.4 kb positive-sense RNA virus belonging to the *family Arteriviridae*, the *order Nidovirales* (Gorbalenya et al., 2006). Comparative genome sequence analysis has revealed that PRRSV has two distinct genotypes, type 1 (European type) and type 2 (North American type) (Benfield et al., 1992; Nelsen et al., 1999). The PRRSV genome consists of at least 10 overlapping open reading frames (ORFs): ORFs 1a, 1b, 2a, 2b, 3, 4, 5a, 5, 6, 7 (Fang and Snijder, 2010; Firth et al., 2011; Johnson et al., 2011; Li et al., 2014; Oh and Lee, 2012; Snijder and Meulenberg, 1998). ORF1a and ORF1b encode replicative enzymes (Fang and Snijder, 2010), of which nsp2 is the largest PRRSV protein and its central region is highly variable with deletions and insertions (Fang et al., 2004; Kim et al., 2010; Yoshii et al., 2008). The key enzymes for PRRSV RNA synthesis are encoded in ORF1b, in particular the viral RNA-dependent RNA polymerase (RdRp, nsp9), which is essential for both genome replication and the synthesis of a nested set of subgenomic (sg) mRNAs (Fang and Snijder, 2010). The GP5 and M proteins, which are encoded by ORF5 and ORF6, respectively, are the major structural proteins of PRRSV. It has been shown that one of the major virulence determinants of PRRSV is located in GP5 (Kwon et al., 2008). As a non-glycosylated membrane protein, M is closely associated with the function of GP5 and likely plays a key role in virus assembly and budding.

The utilization of codon pair in protein coding sequences is highly biased. Some pairs of codons are overrepresented, while other pairs are underrepresented compared to the frequency

* Corresponding author at: State Key Laboratory of Agrobiotechnology, Department of Microbiology and Immunology, College of Biological Science, China Agricultural University, Beijing 100193, China.
E-mail address: whfeng@cau.edu.cn (W.-h. Feng).
[1] These authors contributed equally to this work.

http://dx.doi.org/10.1016/j.virol.2015.07.012
0042-6822/

expected from the usage of the individual codons of these pairs. This phenomenon is termed as codon pair bias (CPB) (Gutman and Hatfield, 1989). Codon-pair bias has been found in every species examined, and it can be quantified statistically (Moura et al., 2007). Although it is not clear how codon pair preference is formed (Buchan et al., 2006), the codon pair usage in an open reading frame can influence the gene expression (Irwin et al., 1995). It has been shown that synthesizing novel poliovirus and influenza virus to contain underrepresented codon pairs while exactly preserve the codon usage and amino acid sequence, can dramatically attenuate the virus (Coleman et al., 2008, 2011; Mueller et al., 2010; Yang et al., 2013). Recently, a report showed that deoptimization of the major envelope GP5 gene attenuated PRRSV (Ni et al., 2014).

To attenuate the HP-PRRSV strain HV, we redesigned large parts of the coding regions of nsp2, nsp9, GP5 and M using rare codon pairs by a specific de-optimization computer program (Coleman et al., 2008). The program can rearrange synonymous codons to yield rare codon pairs while not altering amino acid sequence. Using chemical synthesis and reverse genetics we constructed and rescued the recombinant HP-PRRSV virus HV-nsp2^{min}, HV-nsp9^{min}, and HV-nsp29^{min}. To be compared with their parental strain HV, the recombinant viruses, especially HV-nsp9^{min} and HV-nsp29^{min} replicated significantly slower *in vitro*. Most importantly, HV-nsp9^{min} and HV-nsp29^{min} were attenuated *in vivo* and pigs vaccinated with HV-nsp29^{min} were completely protected from the lethal challenge with HP-PRRSV strains.

Results

The CPB in pig genome and construction of codon pair de-optimized highly pathogenic PRRS virus

To attenuate the highly pathogenic PRRS virus HV strain by de-optimization of the virus gene codon pair usage, we first analyzed the codon pair usage in the pig genome using the algorithm described before (Coleman et al., 2008). Our analysis revealed that there was a normal distribution between −0.2 to 0.3 for the CPB value of the pig genes (Fig. 1). We then re-coded part coding regions for HV nsp2, nsp9, GP5, and M genes using codon pairs which are under-represented relative to the pig genome through shuffling the synonymous codons without altering amino acid sequence. This resulted in dozens or even hundreds of silent mutations (Table 1), and the CPB values of the re-coded gene sequences were much lower than that of normal pig genes (from −0.04472 to −0.40141 for GP5, −0.04297 to −0.40440 for M, from −0.03984 to −0.40700 for nsp2, and −0.00548 to −0.20000 or −0.40210 for nsp9) (Fig. 1 and Table 1).

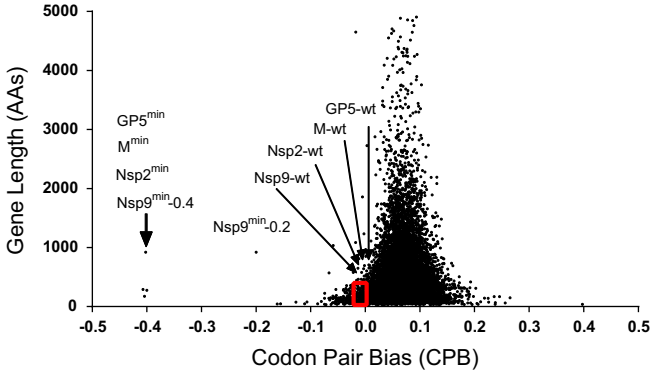

Fig. 1. Calculated codon pair bias (CPB) score for all 14,724 swine genes. Each dot represents the calculated CPB score of a gene plotted against its amino acid length. Underrepresented codon pairs yield negative scores. The CPB of various PRRSV gene segments are indicated by arrows.

The characteristics of the recoded gene segments and the changes of their codon pair bias are summarized in Table 1.

To generate HV virus carrying the de-optimized gene segments, we synthesized and incorporated the rearranged segments into the full-length infectious cDNA construct of HV virus, and the resulted plasmids were then transfected into 293FT cells. At 48 h after transfection, cell culture supernatants were detected for viable virus. Only HV with de-optimized nsp2 (designated as HV-nsp2^{min}) and HV with de-optimized nsp9 (CPB = −0.2) (designated as HV-nsp9^{min} −0.2) yielded viable viruses (Fig. S1), while the other three constructs did not produce any viable virus even after three blind passages of the supernatants from transfected cells. In order to get additional effects of the codon pair de-optimization, we constructed HV-nsp29^{min} plasmid with the de-optimized nsp2 and de-optimized nsp9 (CPB = −0.2), and yielded the de-optimized recombinant virus HV-nsp29^{min} (Fig. S1). For convenience, the virus HV-nsp9^{min} −0.2 was abbreviated as HV-nsp9^{min} in the following studies.

Decreased fitness of the codon pair de-optimized recombinant virus in PAMs

To evaluate and compare the *in vitro* growth characteristics between the recombinant virus HV-nsp2^{min}, HV-nsp9^{min}, HV-nsp29^{min}, and their parental virus HV, we examined their growth kinetics in PAMs infected with an moi of 0.01. These de-optimized viruses did not replicate as well as the wild-type HV (HV-wt). As shown in Fig. 2A, there were hardly any living PAMs existed at 84 h post-infection (hpi) with wild-type HV. However, there was no obvious cytopathic effect observed in PAMs infected with either HV-nsp9^{min} or HV-nsp29^{min} (Fig. 2A). The cytopathic effect induced by the mutant virus HV-nsp2^{min} was only slightly reduced with respect to the wild-type HV (Fig. 2A). These mutated viruses had similar growth curves with the wild-type HV, but they grew much slower than the wild-type HV, and the titers of the de-optimized viruses were lower compared to the wild-type HV at all the time points examined during the replication (Fig. 2B). The titer of HV-nsp2^{min} at 84 hpi was decreased 4 folds compared to wild-type HV, whereas the titer of HV-nsp9^{min} at 84 hpi was much lower by orders of magnitude, up to a factor of 1659. The recombinant virus HV-nsp29^{min} containing both nsp2^{min} and nsp9^{min} replicated as much slowly as HV-nsp9^{min}, suggesting that de-optimization of PRRSV RNA-dependent RNA polymerase nsp9 has much severer effect on virus replication. These results corresponded well with nsp2, nsp9, and GP5 protein and mRNA expression levels analyzed by western blot (Fig. 2C) and RT-PCR (Fig. 2D). Previous studies had hypothesized that attenuation of virus through codon pair bias maybe result from the down-regulation of protein synthesis (Coleman et al., 2011). We therefore analyzed the expression of the wild-type and mutated nsp2 and nsp9 genes cloned into pCMV-myc vector in porcine cell line CRL-2843 using western blot. As shown in Fig. 2E, protein levels of both nsp2^{min} and nsp9^{min} were significantly down-regulated compared to their parental wild-type genes. However, the mRNA expressions of the mutated genes were even slightly higher when compared to their parental wilt-type genes (Fig. 2F). Collectively, these results suggest that codon pair de-optimization of viral genes decreases their protein expressions, leading to the defect in replicative capacity of the mutational viruses relative to their parental virus.

HV-nsp29^{min} and HV-nsp9^{min} was attenuated in pigs

Given that HV-nsp29^{min} was highly attenuated in PAMs, we next investigated its growth phenotype and pathogenesis in pigs to examine whether it was also attenuated *in vivo*. Two groups of 4-week-old healthy conventional pigs were inoculated with either wild-type HV

Table 1
Characteristics of deoptimized PRRSV genome segments

Gene	Coding region[a]	Deoptimized coding region[b]	Wildtype segment			deoptimized segment			Number of silent mutations	Mutant virus viability
			CPB[c]	CpG[d]	UpA[e]	CPB[c]	CpG[d]	UpA[e]		
GP5	13,698–14,300	13,698–14249	−0.04	0.72	0.64	−0.40	1.28	0.86	58	−
M	14,285–14,809	14,285–14659	−0.04	0.76	0.8	−0.40	1.20	1.01	45	−
nsp2	1336–4188	1474–2055	−0.03	0.65	0.54	−0.41	1.06	1.00	95	+
nsp9	7474–9527	7683–9527	−0.01	0.72	0.75	−0.20	0.99	0.91	89	+
						−0.40	1.28	1.13	232	−

[a] Nucleotide position corresponding to PRRSV HV strain (GenBank accession no: JX317648)
[b] Nucleotide position within the HV gene segment that underwent the codon pair deoptimization algorithm.
[c] Codon-pair bias (CPB) of the corresponding sequence.
[d] Ratio of observed dinucleotide frequency to that expected based on mononucleotide composition *i.e.* f(CpG)/f(C)*f(G).
[e] Ratio of observed dinucleotide frequency to that expected based on mononucleotide composition *i.e.* f(UpA)/f(U)*f(A).

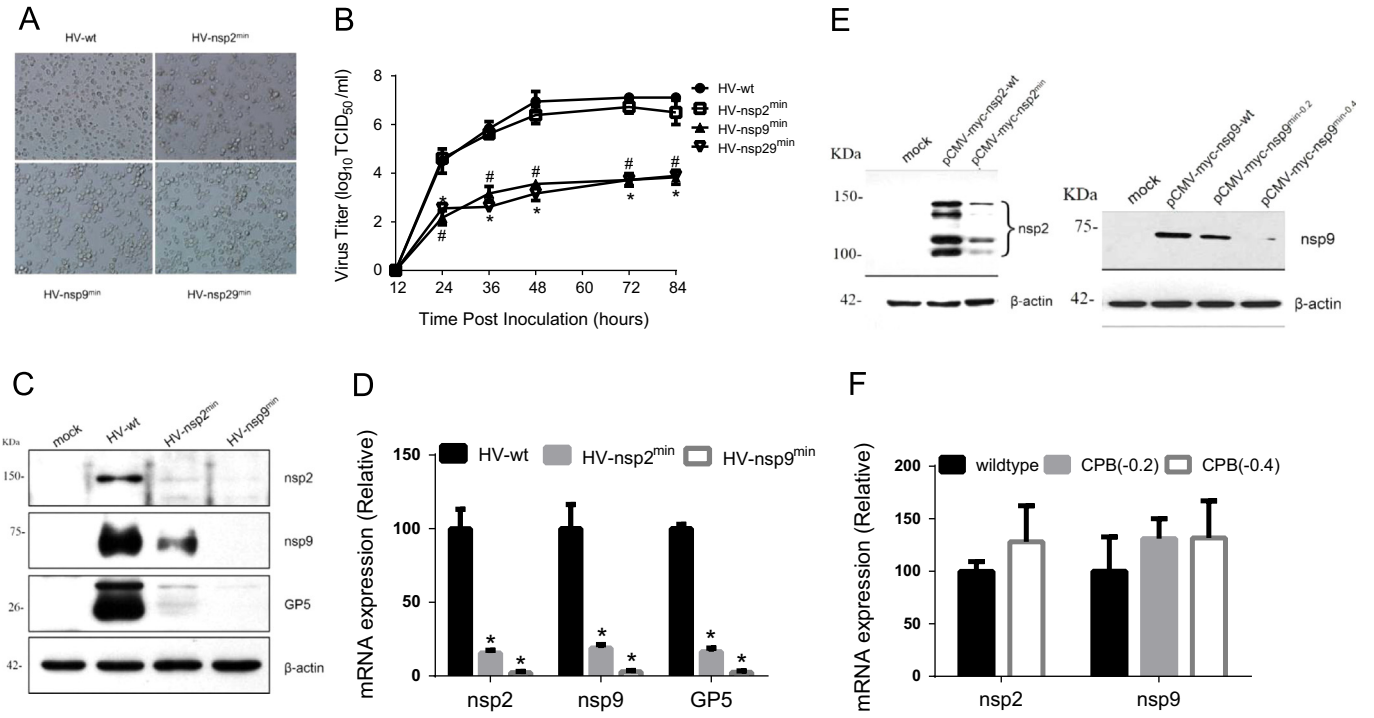

Fig. 2. Recombinant PRRS virus HV-nsp9^{min} and HV-nsp29^{min} grow significantly slower than their parental wild-type HP-PRRSV HV *in-vitro*. PAMs were infected with of either wild-type HP-PRRSV HV, or recombinant PRRS virus HV-nsp2^{min}, HV-nsp9^{min} or HV-nsp29^{min} at an MOI of 0.01. (A) Representative images of cytopathic effects induced by PRRSV at 84 hpi. (B) Supernatants were collected at indicated times and titrated for virus using $TCID_{50}$ method. (C and D) PAMs were infected with HV-wt, HV-nsp2^{min}, or HV-nsp9^{min} at a multiplicity of infection (MOI) of 0.01. At 84 h post-infection, cell lysates were subjected for Western blot to examine the levels of nsp2, nsp9, GP5 and β-actin (C), and total RNAs were extracted from cells and qPCR was performed for analyzing the expression of nsp2, nsp9 and GP5 (D). (E) Analysis of nsp2 and nsp9 protein expression in transfected cells. CRL2843 cells were transfected with 200 ng pCMV-nsp2-wt, pCMV-nsp2^{min}, pCMV-nsp9-wt, pCMV-nsp9$^{min-0.2}$ or pCMV-nsp9$^{min-0.4}$ individually, and Western blot (WB) analysis of proteins extracted from whole cell lysates was carried out with myc or β-actin antibodies. β-actin was used to indicate equal protein loading. (F) RNA expression was analyzed by real-time PCR. The experiments were performed in triplicate, and differences were considered to be statistically significant if $p < 0.05$. * and #, statistically significant difference between each of the recombinant viruses and the wild-type virus at the time point indicated.

(5 pigs) or HV-nsp29^{min} (8 pigs) intranasally with a dose of 2 ml × 10^5 $TCID_{50}$/ml (To get higher virus titer for HV-nsp29^{min}, HV-nsp29^{min} virus was concentrated by ultra-centrifugation), and the pigs were monitored for disease symptoms continuously for 34 days. Pigs infected with the wild-type HV strain quickly developed PRRS disease including coughing, dyspnoea, anorexia, chemosis, shivering, lameness and skin cyanopathy. High body temperatures (> 40 °C) could be detected as early as 4 days post-inoculation (p.i.), and remained higher than 40.5 °C from then (Fig. 3A). All 5 pigs died within 12 days p.i. (Fig. 3B). However, the de-optimized virus HV-nsp29^{min} only induced transient elevated body temperatures, which did not exceed 39.5 °C during 8–14 days p.i., and then fell into normal temperature range (Fig. 3A). All pigs in HV-nsp29^{min} inoculated group remained healthy and did not show clinical symptoms (Fig. 3B). Serum samples from pigs infected with the recombinant virus HV-nsp29^{min} had significantly lower viral load than those from pigs infected with the wild-type HV at all times detected, although the two viruses had similar growth kinetics *in vivo* (Fig. 3C). At 4 days p.i., the titers of HV in serum samples quickly increased to 10^6 $TCID_{50}$/ml when less than 10^3 $TCID_{50}$/ml of HV-nsp29^{min} could be detected. The wild-type HV achieved maximum titers at around 12 days p.i., while the variant HV-nsp29^{min} achieved maximum titers at about 14 days p.i. However, there was an ~10,000-fold difference in the titers between the two viruses. The peak titer of wild-type HV was about $10^{7.4}$ $TCID_{50}$/ml, whereas for HV-nsp29^{min}, the peak was only $10^{3.4}$ $TCID_{50}$/ml. Moreover, at 34 days p.i., HV-nsp29^{min} was eventually not detectable. To further determine the replicative capacity and pathogenicity of HV-nsp29^{min} *in vivo*, the pigs infected with wild-type HV were necropsied when they were dying while 3 of the 8 pigs inoculated with HV-nsp29^{min} were euthanized at two weeks p.i. Multiple tissues were collected for virus RNA quantification and histopathological analysis. Quantitative RT-PCR revealed that pigs infected with HV-nsp29^{min} had significantly lower viral RNA loads in

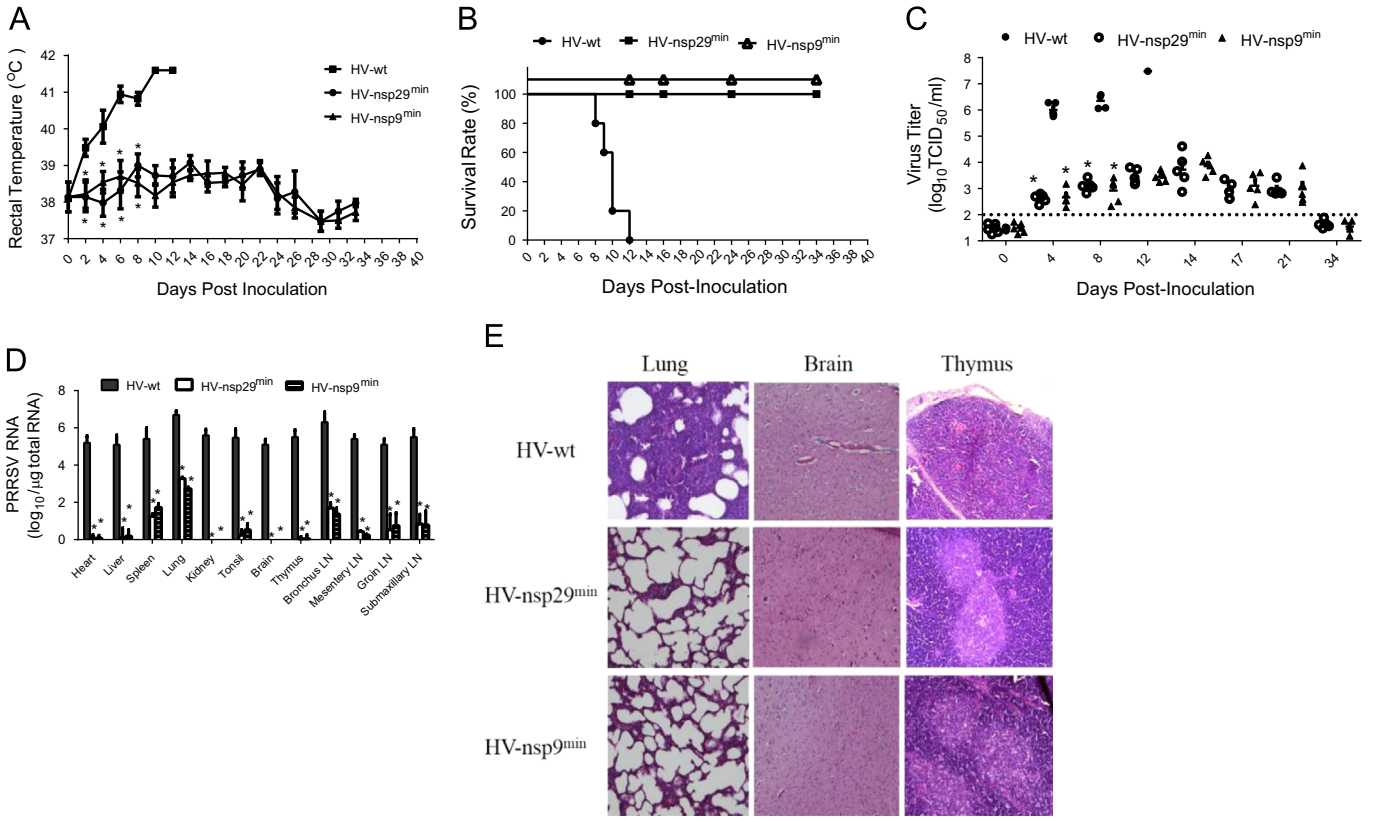

Fig. 3. HV-nsp29^{min} and HV-nsp9^{min}was attenuated *in vivo*. Pigs were intranasally inoculated with HV, HV-nsp29^{min} or HV-nsp9^{min} at a dose of 2×10^5 $TCID_{50}$. (A) Rectal temperature was measured every two days for each group of pigs ($n=5$) after virus infection. (B) Survival curves of pigs in each group. (C) Analysis of viral load in serum from each group of pigs at indicated times post-infection. The limit of serum virus titers detection is indicated in dashed line. (D) Virus RNA load analysis for tissues collected when pigs were dying or necropsied two weeks post-infection. LN, lymph node. (E) Histological examination of tissues collected when pigs were dying or necropsied two weeks post-infection. Differences were considered to be statistically significant if $p < 0.05$.

different tissues (Fig. 3D) by a factor of orders of magnitude, from 3.5 to 5.6, including heart, liver, spleen, lung, kidney, tonsil, brain, thymus, and some lymph nodes. Although the level of viral RNA loads in the lung was higher compared to the other tissues in HV-nsp29^{min} infected pigs, it was still significantly lower than that in the lungs of pigs infected by wild-type HV by a factor up to 3.3 orders. Pathology evaluation revealed that there were severe interstitial pneumonia, thymic atrophy, enlarged lymph nodes, and blood spots on the kidney in HV infected pigs. However, for HV-nsp29^{min} infected pigs, no obvious pathological damages were observed. Histological examinations shown in Fig. 3E further confirmed severe histopathologic damages in all wild-type HV infected pigs including severe proliferative interstitial pneumonia with alveolar septa thickened by lymphomononuclear infiltration in the lung, and severe degrees of vasculitis characterized by massive lymphomononuclear infiltration surrounding perivascular cuffing in the brain. HV-infected pigs had thymic lesions of cortical involution, causing a poor demarcation between the cortical and medullary zones. However, no obvious histopathologic damages other than mild interstitial pneumonia were observed in HV-nsp29^{min} infected pigs. We also infected pigs with HV-nsp9^{min} and got similar results as HV-nsp29^{min}. Taken together, our results demonstrated that the codon pair de-optimized virus HV-nsp9^{min} and HV-nsp29^{min} had decreased replicative capacity, and thus were attenuated in pigs.

HV-nsp29^{min} immunization protected pigs from HP-PRRSV strain challenges

We next investigated whether vaccination with HV-nsp29^{min} could protect pigs from wild-type HP-PRRSV challenges. Groups of four pigs were vaccinated with HV-nsp29^{min} with a dose of 2 ml of 10^5 $TCID_{50}$/ml, or mock vaccinated with RPMI 1640. Thirty-four days after vaccination, the vaccinated pigs were challenged with the wild-type HP-PRRSV strain HV (belonging to the 2006 to 2008 HP-PRRSV isolate subgroup) or another HP-PRRSV strain JX virus (belonging to the 2009 to 2010 HP-PRRSV isolate subgroup) (Wang et al., 2012) at a dose of 2 ml of 10^6 $TCID_{50}$/ml. The mock vaccinated pigs in the control group were challenged with the wild-type HP-PRRSV strain HV. Viremia was cleared in each of the pigs when challenge was performed at 34 days post-vaccination. All pigs were necropsied at 14 days post-challenge.

As with the original infections, we monitored disease symptoms, the body temperature, and survival of the pigs for 14 days after the challenge. Vaccination of the pigs with HV-nsp29^{min} could completely protect pigs from both wild-type HP-PRRSV strain HV and another HP-PRRSV strain JX lethal challenges and none of the pigs died (Fig. 4A) The vaccinated animals did not show any clinical signs throughout the experiment, and their body temperature remained in the normal range until the experiment finished (Fig. 4B), while the body temperature of mock vaccinated animals rapidly rose above 40 °C (Fig. 4B), and all of them died within 14 days post-challenge (Fig. 4A). All the mock vaccinated animals challenged with HP-PRRSV strain JX at a dose of 2 ml of 10^6 $TCID_{50}$/ml had similar symptoms and died within 14 days. For pigs challenged with the homologous wild-type strain HV, the serum viral load in the vaccinated pigs was below10^2 $TCID_{50}$/ml, which was significantly reduced by more than 10,000-fold compared to the mock vaccinated pigs at 4 and 8 dpc (Fig. 4C). For pigs challenged with the other HP-PRRSV strain JX, the reduction of the serum viral loads were also more than 10,000-fold compared to that in the mock vaccinated pigs at 4 and 8 dpc, similar to that in pigs challenged with the homologous wild-type HV strain (Fig. 4C). The viral RNA loads in

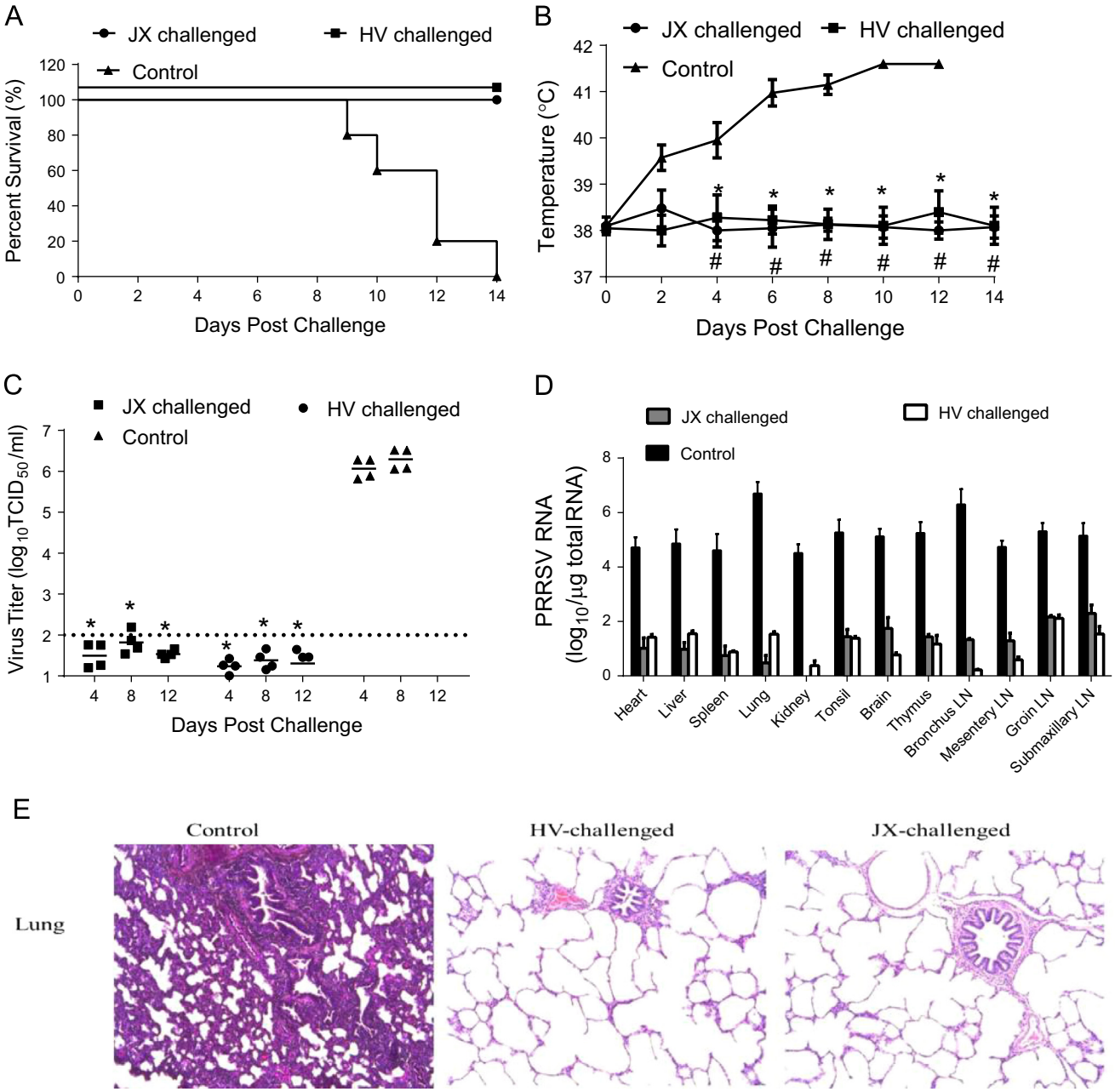

Fig. 4. Pigs immunized with HV-nsp29^{min} are protected from wild-type HP-PRRSV HV and JX isolates' lethal challenges. Pigs were immunized with HV-nsp29^{min} at a dose of 2×10^5 $TCID_{50}$/ml and challenged with either HV or JX at 2×10^6 $TCID_{50}$/ml at 34 days post-immunization. Pigs in the control group (not immunized) were challenged with HV at 2×10^6 $TCID_{50}$/ml. Survival of pigs (A), Rectal temperatures (B), and virus titers in serum samples (C) were monitored. (D) Virus load analysis for tissues collected when pigs were dying or necropsied two weeks post-challenge. LN, lymph node. (E) Histological examination of lung collected when pigs were dying or necropsied two weeks post-challenge. Differences were considered to be statistically significant if $p < 0.05$.

tissues from vaccinated pigs challenged with homologous wild-type HP-PRRSV strain HV or another HP-PRRSV strain JX were comparable, and both were numbers of orders decreased compared to that in control group pigs, especially in the lung, which is the primary target organ of PRRSV infection. The viral titers in pigs vaccinated with HV-nsp9^{min} were about 5–6 orders of magnitude lower than that in control group (Fig. 4D). Histological examination showed that there were limited pathological changes in lungs of the vaccinated pigs, whereas there was severe interstitial pneumonia in un-vaccinated pigs (Fig. 4E). Collectively, our results indicated that vaccination of the pigs with HV-nsp29^{min} could completely protect the animals from HP-PRRSV isolate lethal challenges.

Neutralization antibody and CD8$^+$ T cell response induced by the HV-nsp29^{min} variant

Live attenuated vaccines in general depend on a limited, yet safe, degree of replication within the host to stimulate the immune system. Since HV-nsp29^{min} had a reduced replicative capacity and was attenuated in pigs, we also investigated whether the limited replication of HV-nsp29^{min} could elicit protective immune response in pigs against HP-PRRSV.

To investigate if the protective immune response is induced by HV-nsp29^{min}, serum neutralization assay and intracellular IFN-γ flow cytometric analysis were performed. As shown in Fig. 5A, at 8 days post-vaccination, neutralization antibody against PRRSV

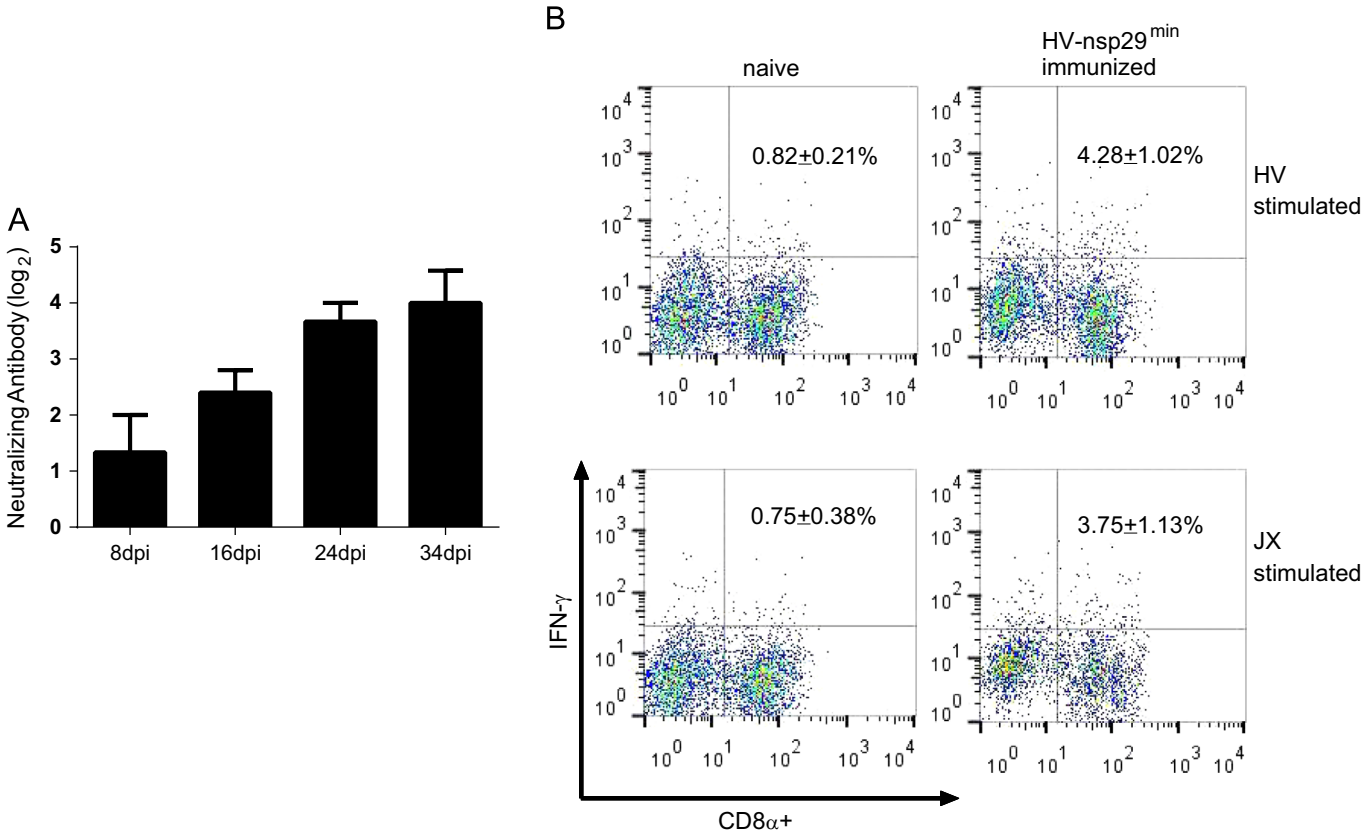

Fig. 5. Vaccination with HV-nsp29^{min} elicits both humoral and cell-mediated immune responses. (A) Neutralizing antibody response at different time post-HV-nsp29^{min} vaccination was determined by serum neutralization assay. (B) IFN-γ-secreting CD8α^{+} T cells were determined by flow cytometric analysis at 34 days post-vaccination following *in vitro* re-stimulation with HP-PRRSV isolate HV or JX.

was about 1:2, and the titers of neutralization antibody increased along with the time. At 34 days post-vaccination when challenge was performed, the titers increased to about 1:16. IFN-γ is considered to be a key cytokine in CD8^{+} T cell response, and serves as an indicator for the cell mediated responses. Therefore, we examined the levels of IFN-γ in CD8^{+} T cells from immunized pigs when stimulated with HP-PRRSV strains HV and JX *in vitro*. As shown in Fig. 5B, vaccination with HV-nsp29^{min} significantly induced IFN-γ expressing CD8^{+} T cells (from 0.82 to 4.28% for HV and 0.75 to 3.75% for JX), suggesting that a significant cell-mediated immune response against HP-PRRSV is induced by HV-nsp29^{min} vaccination. Collectively, these results indicated that the attenuated HV-nsp29^{min} possessed the ability to elicit decent levels of neutralization antibody and CD8^{+} T cell responses against HP-PRRSV infection.

Discussion

It has been known since 1989 that codon pair usage is biased (Gutman and Hatfield, 1989) and this phenomenon has previously been studied primarily by informatics (Fedorov et al., 2002; Moura et al., 2007). Coleman et al. reported that recoding poliovirus and influenza virus with underrepresented codon pairs relative to human genome caused poor translation and induced attenuation in poliovirus and influenza virus (Coleman et al., 2008; Mueller et al., 2010; Yang et al., 2013). Here, we successfully attenuated HP-PRRSV through recoding virus nsp2 and nsp9 genes with under-represented codon pairs relative to pig genome, while encoding precisely the same amino acid sequences as wild-type virus, thereby generating viral variants HV-nsp2^{min}, HV-nsp9^{min}, and HV-nsp29^{min}. And importantly, our data showed that HV-nsp9^{min} and HV-nsp29^{min} were significantly attenuated both *in vitro* and *in vivo*, and pigs vaccinated with HV-nsp29^{min} were protected from HP-PRRSV strain lethal challenges.

Atypical PRRS caused by HP-PRRSV is a devastating disease for swine industry in China and Southeast Asia. To date, three empirical attenuated vaccines specific for HP-PRRSV are commercialized in China, including JXA1-R, HuN4-F112 and TJM-F92. All of these vaccines were obtained by passaging virulent PRRSV isolates on the African green monkey kidney epithelial cell line Marc-145 (Han et al., 2009; Leng et al., 2012; Tian et al., 2009; Yu et al., 2012). Disadvantages of current PRRSV MLVs include that they have the risk of reversion to virulence, as well as that pigs vaccinated with MLVs cannot be distinguished from those naturally-infected with field strains of PRRSV. The gene stability of live attenuated virus is critical as they could infect and replicate in the host, and small chance of the attenuated vaccine strain's reversion to virulence may result in virus spreading caused by vaccine inoculation. Hence, the use of live vaccines with PRRSV strains prone to mutations has raised concern about safety, especially since a vaccination program led to an epidemic of American type 2 PRRSV in the previously unaffected Danish pig population as a result of reversion to virulence of the vaccine strain (Nielsen et al., 2001). In the present study, the attenuation resulted from hundreds of nucleotide changes across the viral genome, therefore reversion of the de-optimized variant to a virulent form is unlikely, and also the attenuated virus can be easily distinguished from the wild-type virus by PCR. More importantly, co-infection of the vaccine recipient with a naturally circulating wild-type virus could lead to RNA recombination between PRRSV isolates (van Vugt et al., 2001; Yuan et al., 1999). But this is unlikely to produce variants more virulent than the co-infecting virus when the attenuated HV-nsp9^{min} or HV-nsp29^{min} is

used, because the de-optimized segments of the vaccine strain could only "attenuate" any such isolate.

The precise mechanism by which underrepresented codon pairs cause attenuation is still unknown. It has been noticed that introducing the unfavorable codon pairs also increases the number of CpG or UpA nucleotide pairs present in the RNA of the virus (Tulloch et al., 2014). It has long been known that genomes of RNA viruses have low CpG and UpA dinucleotide frequencies (Rima and McFerran, 1997; Rothberg and Wimmer, 1981), as do mammalian coding regions generally (Alff-Steinberger, 1987), a phenomenon which must be advantageous for viruses. Indeed, previous studies have revealed that echovirus 7 with increased frequencies of CpG and UpA show impaired replication kinetics and higher RNA/infectivity ratios compared with wild-type virus. Remarkably, mutants with CpGs and UpAs removed showed enhanced replication and larger plaques, and rapidly outcompeted wild-type virus on co-infections (Atkinson et al., 2014). If the CpG or UpA content is raised in the poliovirus polyprotein encoded with synonymous rare CpG- and UpA-rich codons, the resulting variants are either debilitated in growth (Burns et al., 2009; Atkinson et al., 2014) or nonviable (Mueller et al., 2006). In our studies, we found that the recoded segments within the GP5^{min}, M^{min}, nsp2^{min} and nsp9^{min} genomes also present with an increased frequency of CpG and UpA dinucleotides (Table 1). It has been proposed that increased CpG may activate the innate immune response in some tissue culture cells, thereby reducing viral replication (Burns et al., 2009; Atkinson et al., 2014). Further investigation is needed to confirm whether the increased CpG activates innate immune response in PAMs. Nevertheless, despite the underpresented codon pairs and increased CpG and UpA frequencies within nsp2^{min}, the recombinant virus HV-nsp2^{min} did not show obvious replication default, implying that other factors, such as synthesis of the polyprotein, its processing, misfolding, stability and/or parameters that have yet to be investigated may also be related to the attenuation of the codon pair deoptimized recombinant virus.

The protective immune response in pigs infected with wild-type PRRSV is unusual due to a weak and delayed production of neutralizing antibodies (NA) as well as a weak and slow gradual development of a cell-mediated immune response (CMI) (Darwich et al., 2010). In the present study, NA was about 1:2 at 8 day post-immunization, and its titer was up to 1:16 at 24 day post-vaccination. It was reported that pigs with a serum NA titer of 1:8 did not develop viremia (Lopez and Osorio, 2004; Osorio et al., 2002), suggesting that a vaccine capable of inducing NA titres of 1/8 or higher should prevent clinical disease and be a key tool in eradication of PRRSV. And it is true that in the present study, PRRSV was undetectable in serum at 34 days post-infection. In a recently published paper (Galliher-Beckley et al., 2015), the authors showed that pigs vaccinated with JXA1-R, a commercial vaccine modified from a HP-PRRSV strain, produced measurable titers of neutralizing antibody against JXA1-R (>12), and HV-PRRSV (HP-PRRSV strain) (>8), and NADC-20 (the most virulent strains circulating in North America) (>4) 28 days post-vaccination, and were protected from the challenge with DADC-20. In addition, to assess PRRSV specific T-cell response in pigs, we analyzed the IFN-γ positive CD8$^+$ T cells at 34 days post-infection. Recall response showed that about 4.28% and 3.75% of CD8$^+$ T cells were IFN-γ positive after being re-stimulated with homologous HV and another HP-PRRSV JX isolate, respectively, suggesting that effective cell-mediated immune response was also induced. In the process of de-optimizing virus codon pair bias, the amino acid sequence of viral gene is precisely conserved. Therefore, vaccines produced in this way express the entire wild-type repertoire of antigenic sites and would have the maximum chance to induce both cellular and humoral immunity against all epitopes. As the high gene homology shared among the different HP-PRRSV strains, the attenuated virus variant could provide pigs with complete protection against subsequent both HP-PRRSV lethal challenges. The possible reasons for HV-nsp9^{min} and HV-nsp29^{min} to be highly attenuated *in vivo* could be that 1) HV-nsp9^{min} and HV-nsp29^{min} replicate much slower in porcine macrophages, and therefore HV-nsp9^{min} and HV-nsp29^{min} infections could not cause much damage to macrophages, and subsequently induce high quality innate immune responses; 2) HV-nsp9^{min} and HV-nsp29^{min} infection does not cause pathologic effects on thymus, which is the site for T cell development, and other tissues and organs such as bone marrow (data not shown). Thus, immunization with HV-nsp29^{min} infection induced relatively high quality immune response and protected pigs from lethal challenge with either homologous HP-PRRSV isolate or different isolate. However, further investigation is needed to study the underlying mechanisms for the attenuation.

Taken together, the synthesized codon pair de-optimized PRRSV HV-nsp9^{min} and HV-nsp29^{min} were significantly attenuated and had potential to be used as vaccine candidates against HP-PRRSV. Our results further ascertain that the strategy "de-optimization of codon pair bias to attenuate virus" pioneered by Coleman et al. (2008) could be used to make modified live vaccines.

Materials and methods

Cells and viruses

Porcine alveolar macrophages (PAMs) were obtained by post-mortem lung lavage of 8-week-old specific pathogen free (SPF) pigs, and maintained in RPMI 1640 supplemented with 10% FBS and penicillin/streptomycin. CRL-2843 (also referred as CD4/21) cells, a porcine alveolar macrophage cell line, were maintained in RPMI 1640 medium supplemented with 10% FBS and penicillin–streptomycin.

The HP-PRRSV strain HV (GenBank accession no: JX317648) and JX (GenBank accession no: JX317649), were propagated in PAMs. Virus preparations were titrated on PAMs and then stored at −80 °C. The full length infectious cDNA clone of HV in eukaryotic expression vector pcDNA3.1 (+) was constructed and kept by our lab (data not published).

Calculation of codon pair bias (CPB) in pig genome and design of codon pair de-optimized PRRS virus

Based on the previous studies (Coleman et al., 2008), the CPB for an entire open reading frame has been defined as the arithmetic mean of the individual codon pair scores (CPS). The CPS of each codon pair is the natural log of the ratio of the observed over the expected number of occurrences over all coding regions in the genome. We calculated the CPS value for each of the 3721 codon pairs in pig genome as described before (Coleman et al., 2008), and the results could be found in Supplementary Table 1. A positive CPS means that the given codon pair is statistically over-represented, while a negative CPS value signifies that the pair is statistically under-represented in the pig genome. We then analyzed the CPB for 16,174 pig genes (download from NCBI, in November 2011), and the calculated results were shown in Fig. 1A positive CPB indicates a prevalent use of overrepresented codon pairs, while a negative CPB represents the predominant use of underrepresented codon pairs. The CPBs of part of open reading frames of nsp2, nsp9, GP5 and M, corresponding to nucleotides 1474 to 2055, 7683 to 9527, 13,698 to 14,249, and 14,285 to 14,659 of the viral genome, respectively, were calculated as above. We then shuffled the existing codons among the corresponding gene segment so that the CPB can be decreased. All of the codon

changes were synonymous: that is, none of them introduces any amino acid change. The CpG and UpA dinucleotide frequencies in the manipulated sequences was performed using the program Sequence Mutate in version 1.2 of the SSE package (Simmonds, 2012). The precise extent of recoded sequence for each target segment and the resulting changes in codon-pair bias were summarized in Table 1. The codon pair de-optimized gene sequences were synthesized *de novo* chemically (Nanjing GenScript, China), and appropriate restriction sites were included at both terminals of the segments. Then, the codon pair de-optimized segment was cloned into the full length cDNA clone of HV to replace the respective wild-type counterpart sequence. We constructed recombinant HV cDNA clone and yielded HV-nsp2^{min}, HV-nsp9^{min}, HV-GP5^{min}, HV-M^{min} as well as HV-nsp29^{min} plasmids in pcDNA3.1 downstream of CMV T7 promoter.

In vitro transfection and rescue of recombinant viruses

To rescue the infectious codon pair de-optimized PRRS viruses from the recombinant DNA-launched infectious clones, we transfected the plasmids HV-nsp2^{min}, HV-nsp9^{min}, HV-GP5^{min}, HV-M^{min} and HV-nsp29^{min} directly into 293FT cells individually (Wang et al., 2014). Cell culture supernatant obtained at 48 h post-transfection was inoculated on primary cultured PAMs and immunofluorescence assay was performed for virus detection as described previously (Fig. S1) (Gao et al., 2013). Briefly, cells were fixed with cold methanol-acetone (1:1) for 10 min at 4 °C, washed with phosphate-buffered saline (PBS), and then blocked with 5% normal goat serum for 30 min at room temperature. After blocking, cells were stained with anti-PRRSV N protein monoclonal antibody SDOW17 (1:10,000; Rural Technologies), or an isotype control antibody for 60 min at room temperature. Cells were then washed and incubated with FITC-conjugated goat anti-mouse IgG (H+L) (1:2000, Jackson ImmunoResearch) for 60 min at 37 °C. After three washes in PBS, cells were counter-stained with DAPI and examined by fluorescence microscopy. The rescued virus was designated as HV-nsp2^{min}, HV-nsp9^{min} or HV-nsp29^{min}.

Growth characterization of the recombinant virus in vitro

To analyze the growth characteristics of the recombinant virus *in vitro*, one-step growth curves were obtained by infecting a monolayer of PAMs with a given virus. Confluent monolayers of PAMs seeded in 6-well plates were infected with the wild-type virus HV and three rescued recombinant viruses HV-nsp2^{min}, HV-nsp9^{min}, and HV-nsp29^{min} at an MOI of 0.01 for 2 h at 37 °C, and then the viral inoculum was removed. Cells were then washed 3 times with PBS and incubated at 37 °C for 12, 24, 36, 48, 72, and 84 h. The titers of virus harvested at these time points were determined on PAMs and quantified as 50% tissue culture infective doses ($TCID_{50}$). At 84 h post-infection, cell lysates were also subjected for Western blot to examine the levels of nsp2, nsp9, GP5 and β-actin, and total RNAs were extracted from cells and qPCR was performed for analyzing the expression of nsp2, nsp9 and GP5. All *in vitro* experiments were performed in triplicate.

Table 2
Primers used for cloning nsp2 and nsp9 gene.

Primer	Sequence (5′–3′)
Nsp2f	GA AGATCT CTGCCGGAAAGAGAGCAAGGAAAAC
Nsp2r	GG GGTACC CTACCCTGAAGGCTTGGAAATTTG
Nsp9 (7474–7614) f	GTTGGCATATGGCCGCCAAGCTTTCC
Nsp9 (7474–7614) r	GGCTAGCAGGTTGAGACACTGCTCCT
Nsp9 (7593–9526) f	GCAGTGTCTCAACCTGCTAGCCGCCAGC
Nsp9 (7593–9526) r	CCGGATCCTTACTCATGATTGGACCTGAGTTTTTCC

Analysis of wild-type and codon pair de-optimized nsp2, and nsp9 gene expression in transfected cells using Western blot and real-time PCR

The cDNA sequences encoding wild-type and codon pair de-optimized nsp2 and nsp9 were cloned into pCMV-N-myc vector. The ORF1a/ORF1b ribosomal frame shift site was removed as described before (Gao et al., 2013). Briefly, nucleotides T-7600 and A-7602 were mutated to C, and a nucleotide C was inserted between A-7604 and C-7605. Primers were listed in Table 2. CRL2843 cells in 6-well plates were transfected with 200 ng of each of the plasmids encoding the wild-type and codon pair de-optimized nsp2 and nsp9 genes. Cells were harvested with RIPA lysis buffer supplemented with protease inhibitors at 18 h post-transfection. The proteins were resolved by SDS-PAGE, and analyzed by western blot with antibodies against myc (1:1000, Santa Cruz Biotechnology) and β-actin (1:5000; Sigma, St. Louis, MO) and HRP-conjugated secondary antibodies (1:10,000, Santa Cruz Biotechnology). The antibodies were visualized using the ECL reagent according to the manufacturer's instructions. RNA was also harvested for nsp2 and nsp9 gene expression analysis using real-time PCR at 18 h post-transfection (hpt). Real-time PCR was performed using primers specific for nsp2 and nsp2$^{-0.4}$ mutant (forward 5′CTCGTTTCCCATCTCCCTATT3′, and reverse 5′ACGCCGAGAAGACCCAGA3′), nsp9 and nsp9$^{-0.2}$ mutant (forward 5′CTCGTGGTTGGGATAGCG3′, and reverse 5′GGACAAG AAGAACGGTGGG3′), and nsp9$^{-0.4}$ mutant (forward 5′GCCGAG GCTACTAAAGAGGA3′, and reverse 5′GGTATGTCTCCGAACCGTGTA3′).

Pathogenicity study of the recombinant virus HV-nsp29^{min} and HV-nsp9^{min} in vivo

To determine and compare the virulence of recombinant virus HV-nsp29^{min}, HV-nsp9^{min} and the parental virus in pigs, we obtained 4-week-old healthy conventional Large White–Dutch Landrace crossbred pigs from a pig farm that was negative for PRRSV and PCV2 infections. All pigs were further confirmed to be PRRSV and PCV2 antibodies free by using commercial enzyme-linked immunosorbent assay (ELISA) kits (Idexx Lab., and Ingenasa). PRRSV, classical swine fever virus (CSFV), PCV2, and pseudorabies virus (PRV) were also confirmed to be free using PCR or RT-PCR. A total of 21 pigs were randomly divided into 3 groups, and each pig was infected by intranasal inoculation with 2 ml of 10^5 $TCID_{50}$/ml of virus. The control group of 5 pigs was inoculated with wild-type HP-PRRSV strain HV, and the other two groups (8 pigs each) were inoculated with the codon pair de-optimized virus HV-nsp29^{min} and HV-nsp9^{min}, respectively. The animals were observed daily for clinical signs including coughing, dyspnoea, anorexia, diarrhea, lameness, and shivering. Rectal temperatures were measured every other day for 34 days post-inoculation (dpi). Serum was collected at 0, 4, 8, 12, 17, 25 and 34 dpi for the detection of viral titer by quantitative RT-PCR, and known amounts of serially diluted *in-vitro* transcript virus cDNA were used to generate a standard curve for each plate run (Zuckermann et al., 2007). Three pigs in each of the HV-nsp29^{min} and HV-nap9^{min} infected groups were necropsied at 14 days post-inoculation, while the other five pigs were necropsied at 34 dpi when the experiment was finished. Pigs in the control group experiencing severe disease symptoms were necropsied at any time when they were dying. At necropsy, tissues were collected from each pig for histological examination and for quantification of viral-RNA loads.

Challenge-and-protection study in pigs vaccinated with the recombinant virus HV-nsp29^{min}

For vaccination experiments, twelve pigs were randomly divided into three groups (4 pigs/each group). Two groups of pigs

were vaccinated with HV-nsp29^{min} virus at a dose of 2 ml*10^5 $TCID_{50}$/ml intranasally, while pigs in the control group were mock vaccinated with RPMI 1640. Serum samples were collected at 8, 16, 24 and 34 days post-vaccination (dpv) for the determination of the neutralization antibody titers. Whole blood samples were also collected for $CD8^+$ T cell response analysis at 34 dpv. At 34 dpv, the vaccinated pigs were then challenged intranasally with 2 ml of 10^6 $TCID_{50}$/ml of either the HP-PRRSV HV strain or the HP-PRRSV JX strain, while the control group was challenged with the HP-PRRSV HV strain. Clinical signs were monitored daily as above and rectal temperature was measured every other day for 14 days post-challenge (dpc). Serum samples were collected at 4, 8 and 12 dpc for the detection of viral RNA by quantitative RT-PCR. At 14 dpc, all pigs were necropsied, and tissues were collected for histological examination and viral-RNA load quantification.

RNA extraction and real-time PCR

Total RNA was extracted using Trizol Reagent (Invitrogen) and 500 ng RNA was used for cDNA synthesis using M-MLV (Promega). Real-time PCR was performed using specific primers for PRRSV N protein gene (forward AATAACAACGGCAAGCAGCA, and reverse GCACAGTATGATGCGTCGGC) and GP5 protein gene (forward 5′CTCACCACCAGCCATTTCCT3′, and reverse 5′TGCAGTTCTTCG CAAGCCTA3′) on ABI viiA7 Real-Time PCR System using the Real-Time SYBR master mix kit (TAKARA) following the manufacturer's introductions. For each experiment, a standard curve was generated using serially diluted PRRSV standard of 10^0–10^7 $TCID_{50}$/ml.

Serum neutralization assay

Serum neutralization assay was performed as described before (Ostrowski et al., 2002). Briefly, serial 2-fold dilutions of 56 °C heat-inactivated serum samples were incubated with 100 $TCID_{50}$ of HP-PRRSV HV strain in RPMI 1640 containing 10% FBS for 60 min at 37 °C. Then, the mixtures were added to PAMs in 96-well plates which had been cultured for 24 h prior to use. After incubation for another 24 h, immunofluorescence assay for PRRSV detection was performed. Neutralization titers were interpreted as the reciprocal of the highest dilution that showed 90% reduction or greater in the number of the fluorescent foci.

Intracellular IFN-γ flow cytometric analysis

Peripheral blood leukocytes were prepared as described previously (Graham et al., 2012) and stimulated with PRRSV antigen (10 μg/ml) for 6 h at 37 °C. Brefeldin A (10 μg/ml, BD Bioscience) was added to block cytokine release for a further 2 h. Then the cells were stained with anti-CD8α-FITC or isotype control (AbD-serotec) for 30 min at 4 °C. After washing, cells were fixed with 4% paraformaldehyde and permeabilized with 0.1% saponin, and then stained with anti-IFN-γ-RPE or isotype control (AbDserotec) overnight at 4 °C. Cells were washed and then analyzed by flow cytometry. Data were acquired using a FACS Calibur (BD Bioscience) and analyzed using FlowJo software.

Statistical analysis

All experiments were performed with at least three independent replicates. Results were analyzed using *Student's t-test*. Differences were considered to be statistically significant if the p value was less than 0.05. The data were analyzed using GraphPad Prism 5.0.

Acknowledgment

We thank Dr. Weiquan Liu (China Agricultural University, China) for his help for the construction of the infectious cDNA clone. The paper was supported by the Research Fund for the Doctoral Program of Higher Education of China (Grant no. 20130008110028) and the State Key Laboratory of Agrobiotechnology (Grant nos. 2010SKLAB06-1, 2012SKLAB01-6, and 2013SKLAB1-5).

Appendix A. Supporting information

Supplementary data associated with this article can be found in the online version at http://dx.doi.org/10.1016/j.virol.2015.07.012.

References

Alff-Steinberger, C., 1987. Codon usage in Homo sapiens: evidence for a coding pattern on the non-coding strand and evolutionary implications of dinucleotide discrimination. J. Theor. Biol. 124, 89–95.
Atkinson, N.J., Witteveldt, J., Evans, D.J., Simmonds, P., 2014. The influence of CpG and UpA dinucleotide frequencies on RNA virus replication and characterization of the innate cellular pathways underlying virus attenuation and enhanced replication. Nucleic Acids Res. 42, 4527–4545.
Benfield, D.A., Nelson, E., Collins, J.E., Harris, L., Goyal, S.M., Robison, D., Christianson, W.T., Morrison, R.B., Gorcyca, D., Chladek, D., 1992. Characterization of swine infertility and respiratory syndrome (SIRS) virus (isolate ATCC VR-2332). J. Vet. Diagn. Investig. 4, 127–133.
Buchan, J.R., Aucott, L.S., Stansfield, I., 2006. tRNA properties help shape codon pair preferences in open reading frames. Nucleic Acids Res. 34, 1015–1027.
Burns, C.C., Campagnoli, R., Shaw, J., Vincent, A., Jorba, J., Kew, O., 2009. Genetic inactivation of poliovirus infectivity by increasing the frequencies of CpG and UpA dinucleotides within and across synonymous capsid region codons. J. Virol. 83, 9957–9969.
Coleman, J.R., Papamichail, D., Skiena, S., Futcher, B., Wimmer, E., Mueller, S., 2008. Virus attenuation by genome-scale changes in codon pair bias. Science 320, 1784–1787.
Coleman, J.R., Papamichail, D., Yano, M., Garcia-Suarez Mdel, M., Pirofski, L.A., 2011. Designed reduction of Streptococcus pneumoniae pathogenicity via synthetic changes in virulence factor codon-pair bias. J. Infect. Dis. 203, 1264–1273.
Darwich, L., Díaz, I., Mateu, E., 2010. Certainties, doubts and hypotheses in porcine reproductive and respiratory syndrome virus immunobiology. Virus Res. 154, 123–132.
Fang, Y., Kim, D.Y., Ropp, S., Steen, P., Christopher-Hennings, J., Nelson, E.A., Rowland, R.R., 2004. Heterogeneity in Nsp2 of European-like porcine reproductive and respiratory syndrome viruses isolated in the United States. Virus Res. 100, 229–235.
Fang, Y., Snijder, E.J., 2010. The PRRSV replicase: exploring the multifunctionality of an intriguing set of nonstructural proteins. Virus Res. 154, 61–76.
Fedorov, A., Saxonov, S., Gilbert, W., 2002. Regularities of context-dependent codon bias in eukaryotic genes. Nucleic Acids Res. 30, 1192–1197.
Firth, A.E., Zevenhoven-Dobbe, J.C., Wills, N.M., Go, Y.Y., Balasuriya, U.B., Atkins, J.F., Snijder, E.J., Posthuma, C.C., 2011. Discovery of a small arterivirus gene that overlaps the GP5 coding sequence and is important for virus production. J. Gen. Virol. 92, 1097–1106.
Galliher-Beckley, A., Li, X., Bates, J.T., Madera, R., Waters, A., Nietfeld, J., Henningson, J., He, D., Feng, W., Chen, R., Shi, J., 2015. Pigs immunized with Chinese highly pathogenic PRRS virus modified live vaccine are protected from challenge with North American PRRSV strain NADC-20. Vaccine 33, 3518–3525.
Gao, L., Zhang, W., Sun, Y., Yang, Q., Ren, J., Liu, J., Wang, H., Feng, W.H., 2013. Cryptoporus volvatus extract inhibits porcine reproductive and respiratory syndrome virus (PRRSV) *in vitro* and *in vivo*. PLoS One 8, e63767.
Gorbalenya, A.E., Enjuanes, L., Ziebuhr, J., Snijder, E.J., 2006. Nidovirales: evolving the largest RNA virus genome. Virus Res. 117, 17–37.
Graham, S.P., Haines, F.J., Johns, H.L., Sosan, O., La Rocca, S.A., Lamp, B., Rumenapf, T., Everett, H.E., Crooke, H.R., 2012. Characterisation of vaccine-induced, broadly cross-reactive IFN-gamma secreting T cell responses that correlate with rapid protection against classical swine fever virus. Vaccine 30, 2742–2748.
Gutman, G.A., Hatfield, G.W., 1989. Nonrandom utilization of codon pairs in Escherichia coli. Proc. Natl. Acad. Sci. USA 86, 3699–3703.
Han, W., Wu, J.J., Deng, X.Y., Cao, Z., Yu, X.L., Wang, C.B., Zhao, T.Z., Chen, N.H., Hu, H.H., Bin, W., Hou, L.L., Wang, L.L., Tian, K.G., Zhang, Z.Q., 2009. Molecular mutations associated with the *in vitro* passage of virulent porcine reproductive and respiratory syndrome virus. Virus Genes 38, 276–284.
Irwin, B., Heck, J.D., Hatfield, G.W., 1995. Codon pair utilization biases influence translational elongation step times. J. Biol. Chem. 270, 22801–22806.
Johnson, C.R., Griggs, T.F., Gnanandarajah, J., Murtaugh, M.P., 2011. Novel structural protein in porcine reproductive and respiratory syndrome virus encoded by an alternative ORF5 present in all arteriviruses. J. Gen. Virol. 92, 1107–1116.

Kim, S.H., Roh, I.S., Choi, E.J., Lee, C., Lee, C.H., Lee, K.H., Lee, K.K., Song, Y.K., Lee, O.S., Park, C.K., 2010. A molecular analysis of European porcine reproductive and respiratory syndrome virus isolated in South Korea. Vet. Microbiol. 143, 394–400.

Kwon, B., Ansari, I.H., Pattnaik, A.K., Osorio, F.A., 2008. Identification of virulence determinants of porcine reproductive and respiratory syndrome virus through construction of chimeric clones. Virology 380, 371–378.

Leng, X., Li, Z., Xia, M., Li, X., Wang, F., Wang, W., Zhang, X., Wu, H., 2012. Mutations in the genome of the highly pathogenic porcine reproductive and respiratory syndrome virus potentially related to attenuation. Vet. Microbiol. 157, 50–60.

Li, Y., Treffers, E.E., Napthine, S., Tas, A., Zhu, L., Sun, Z., Bell, S., Mark, B.L., van Veelen, P.A., van Hemert, M.J., Firth, A.E., Brierley, I., Snijder, E.J., Fang, Y., 2014. Transactivation of programmed ribosomal frameshifting by a viral protein. Proc. Natl. Acad. Sci. USA 111, E2172–2181.

Li, Y., Wang, X., Bo, K., Tang, B., Yang, B., Jiang, W., Jiang, P., 2007. Emergence of a highly pathogenic porcine reproductive and respiratory syndrome virus in the Mid-Eastern region of China. Vet. J. 174, 577–584.

Lopez, O., Osorio, F., 2004. Role of neutralizing antibodies in PRRSV protective immunity. Vet. Immunol. Immunopathol. 102, 155–163.

Moura, G., Pinheiro, M., Arrais, J., Gomes, A.C., Carreto, L., Freitas, A., Oliveira, J.L., Santos, M.A., 2007. Large scale comparative codon-pair context analysis unveils general rules that fine-tune evolution of mRNA primary structure. PLoS One 2, e847.

Mueller, S., Coleman, J.R., Papamichail, D., Ward, C.B., Nimnual, A., Futcher, B., Skiena, S., Wimmer, E., 2010. Live attenuated influenza virus vaccines by computer-aided rational design. Nat. Biotechnol. 28, 723–726.

Mueller, S., Papamichail, D., Coleman, J.R., Skiena, S., Wimmer, E., 2006. Reduction of the rate of poliovirus protein synthesis through large-scale codon deoptimization causes attenuation of viral virulence by lowering specific infectivity. J. Virol. 80, 9687–9696.

Nelsen, C.J., Murtaugh, M.P., Faaberg, K.S., 1999. Porcine reproductive and respiratory syndrome virus comparison: divergent evolution on two continents. J. Virol. 73, 270–280.

Neumann, EJ, Johnson, K.J., Mabry, CD, Bush, JW, Seitzinger, EJ, Green, AH, Zimmerman JJ., AL, 2005. Assessment of the economic impact of porcine reproductive and respiratory syndrome on swine production in the United States. J. Am. Vet. Med. Assoc. 227 (3), 385–392.

Ni, Y.-Y., Zhao, Z., Opriessnig, T., Subramaniam, S., Zhou, L., Cao, D., Cao, Q., Yang, H., Meng, X.-J., 2014. Computer-aided codon-pairs deoptimization of the major envelope GP5 gene attenuates porcine reproductive and respiratory syndrome virus. Virology 450, 132–139.

Nielsen, H.S., Oleksiewicz, M.B., Forsberg, R., Stadejek, T., Botner, A., Storgaard, T., 2001. Reversion of a live porcine reproductive and respiratory syndrome virus vaccine investigated by parallel mutations. J. Gen. Virol. 82, 1263–1272.

Nieuwenhuis, N., Duinhof, T.F., van Nes, A., 2012. Economic analysis of outbreaks of porcine reproductive and respiratory syndrome virus in nine sow herds. Vet. Rec. 170, 225.

Oh, J., Lee, C., 2012. Proteomic characterization of a novel structural protein ORF5a of porcine reproductive and respiratory syndrome virus. Virus Res. 169, 255–263.

Osorio, F.A., Galeota, J., Nelson, E., Brodersen, B., Doster, A., Wills, R., Zuckermann, F., Laegreid, W., 2002. Passive transfer of virus-specific antibodies confers protection against reproductive failure induced by a virulent strain of porcine reproductive and respiratory syndrome virus and establishes sterilizing immunity. Virology 302, 9–20.

Ostrowski, M., Galeota, J.A., Jar, A.M., Platt, K.B., Osorio, F.A., Lopez, O.J., 2002. Identification of neutralizing and nonneutralizing epitopes in the porcine reproductive and respiratory syndrome virus GP5 ectodomain. J. Virol. 76, 4241–4250.

Rima, B.K., McFerran, N.V., 1997. Dinucleotide and stop codon frequencies in single-stranded RNA viruses. J. Gen. Virol. 78 (Pt 11), 2859–2870.

Rothberg, P.G., Wimmer, E., 1981. Mononucleotide and dinucleotide frequencies, and codon usage in poliovirion RNA. Nucleic Acids Res. 9, 6221–6229.

Simmonds, P., 2012. SSE: a nucleotide and amino acid sequence analysis platform. BMC Res. Notes 5, 50.

Snijder, E.J., Meulenberg, J.J., 1998. The molecular biology of arteriviruses. J. Gen. Virol. 79 (Pt 5), 961–979.

Tian, K., Yu, X., Zhao, T., Feng, Y., Cao, Z., Wang, C., Hu, Y., Chen, X., Hu, D., Tian, X., Liu, D., Zhang, S., Deng, X., Ding, Y., Yang, L., Zhang, Y., Xiao, H., Qiao, M., Wang, B., Hou, L., Wang, X., Yang, X., Kang, L., Sun, M., Jin, P., Wang, S., Kitamura, Y., Yan, J., Gao, G.F., 2007. Emergence of fatal PRRSV variants: unparalleled outbreaks of atypical PRRS in China and molecular dissection of the unique hallmark. PLoS One 2, e526.

Tian, Z.J., An, T.Q., Zhou, Y.J., Peng, J.M., Hu, S.P., Wei, T.C., Jiang, Y.F., Xiao, Y., Tong, G.Z., 2009. An attenuated live vaccine based on highly pathogenic porcine reproductive and respiratory syndrome virus (HP-PRRSV) protects piglets against HP-PRRS. Vet. Microbiol. 138, 34–40.

Tulloch, F., Atkinson, N.J., Evans, D.J., Ryan, M.D., Simmonds, P., 2014. RNA virus attenuation by codon pair deoptimisation is an artefact of increases in CpG/UpA dinucleotide frequencies 3, e04531eLife 3, e04531.

van Vugt, J.J., Storgaard, T., Oleksiewicz, M.B., Bøtner, A., 2001. High frequency RNA recombination in porcine reproductive and respiratory syndrome virus occurs preferentially between parental sequences with high similarity. J. Gen. Virol. 82, 2615–2620.

Wang, L., Hou, J., Gao, L., Guo, X.K., Yu, Z., Zhu, Y., Liu, Y., Tang, J., Zhang, H., Feng, W.H., 2014. Attenuation of highly pathogenic porcine reproductive and respiratory syndrome virus by inserting an additional transcription unit. Vaccine 32, 5740–5748.

Wang, L., Hou, J., Zhang, H., Feng, W.H., 2012. Complete genome sequence of a novel highly pathogenic porcine reproductive and respiratory syndrome virus variant. J. Virol. 86, 13121.

Yang, C., Skiena, S., Futcher, B., Mueller, S., Wimmer, E., 2013. Deliberate reduction of hemagglutinin and neuraminidase expression of influenza virus leads to an ultraprotective live vaccine in mice. Proc. Natl. Acad. Sci. USA 110, 9481–9486.

Yoshii, M., Okinaga, T., Miyazaki, A., Kato, K., Ikeda, H., Tsunemitsu, H., 2008. Genetic polymorphism of the nsp2 gene in North American type – porcine reproductive and respiratory syndrome virus. Arch. Virol. 153, 1323–1334.

Yu, X., Chen, N., Wang, L., Wu, J., Zhou, Z., Ni, J., Li, X., Zhai, X., Shi, J., Tian, K., 2012. New genomic characteristics of highly pathogenic porcine reproductive and respiratory syndrome viruses do not lead to significant changes in pathogenicity. Vet. Microbiol. 158, 291–299.

Yuan, S., Nelsen, C.J., Murtaugh, M.P., Schmitt, B.J., Faaberg, K.S., 1999. Recombination between North American strains of porcine reproductive and respiratory syndrome virus. Virus Res. 61, 87–98.

Zhou, Y.J., Hao, X.F., Tian, Z.J., Tong, G.Z., Yoo, D., Zhou, T.Q., Li, T., Qiu, G.X., Wei, H.J., Yuan, X.F., T.C., 2008. Highly virulent porcine reproductive and respiratory syndrome virus emerged in China. Transbound. Emerg. Dis. 55, 152–164.

Zuckermann, F.A., Garcia, E.A., Luque, I.D., Christopher-Hennings, J., Doster, A., Brito, M., Osorio, F., 2007. Assessment of the efficacy of commercial porcine reproductive and respiratory syndrome virus (PRRSV) vaccines based on measurement of serologic response, frequency of gamma-IFN-producing cells and virological parameters of protection upon challenge. Vet. Microbiol. 123, 69–85.